

Single-photon multiple ionization forming double vacancies in the $2p$ subshell of argon

P. Linusson*

Department of Physics, Stockholm University, AlbaNova University Center, SE-106 91 Stockholm, Sweden

S. Fritzsche

*Helmholtz-Institut Jena, Fröbelstieg 3, D-07743 Jena, Germany and**Theoretisch-Physikalisches Institut, Friedrich-Schiller-Universität Jena, Max-Wien-Platz 1, D-07743 Jena, Germany*

J. H. D. Eland

*Department of Chemistry, Physical and Theoretical Chemistry Laboratory, Oxford University, South Parks Road,**Oxford OX1 3QZ, United Kingdom and Department of Physics and Astronomy, Uppsala University, Box 516, SE-751 20 Uppsala, Sweden*

M. Mucke and R. Feifel*

Department of Physics and Astronomy, Uppsala University, Box 516, SE-751 20 Uppsala, Sweden

(Received 7 March 2013; published 11 April 2013)

Single-photon ionization leading to two vacancies in the $2p$ subshell of argon is investigated experimentally using the photoelectron time-of-flight magnetic bottle coincidence technique. Three peaks corresponding to the 3P , 1D , and 1S states of the dication are found in the ionization energy range 535 to 562 eV. Multiconfigurational Dirac-Fock calculations were performed to estimate the single-photon double-ionization cross sections. Reasonable agreement between the measured and simulated spectra is found if single and double excitations are taken into account in the wave-function expansion.

DOI: [10.1103/PhysRevA.87.043409](https://doi.org/10.1103/PhysRevA.87.043409)

PACS number(s): 32.80.Aa, 32.80.Fb

I. INTRODUCTION

In the past few decades single-photon double ionization (SPDI), a process where the interaction with a single photon releases two electrons from an atom or molecule, has attracted considerable interest. Experimentally, the most important tool for the study of SPDI has been photoelectron spectroscopy (PES), in particular efficient coincidence techniques such as threshold photoelectrons coincidence (TPESCO) [1] and the time-of-flight magnetic bottle technique [2] used here. The majority of work has focused on double ionization leading to double vacancies in the outer shells of atoms and small molecules (see the recent reviews [3–5] and references therein).

In the past decade the PES coincidence techniques have been applied to SPDI processes involving core vacancies. Core-valence ionization, where one electron is emitted from a (deep) inner shell and one from the valence, has been studied for a range of inner shells and targets [6–12]. Very recently, SPDI leading to atoms and molecules with two vacancies in the core, so-called double core holes (DCH), have been added to the list [13–17]. SPDI in the core of atoms and molecules has a very small cross section, making its detection a formidable challenge to experimentalists. Previously, double vacancies in the core of atoms have been inferred from their decay, as it leads to so-called “hypersatellites” in x-ray fluorescence spectra [18], and Auger electron spectra [19]. Energy analysis of the photoelectrons emitted in DCH formation by SPDI has as yet, to the best of our knowledge, only been achieved using the TOF magnetic bottle coincidence technique.

With the exception of [13,16] previous photoelectron spectroscopy studies on SPDI leading to two vacancies in the core have mainly concerned the formation of hollow species. Here we present results on the formation of two vacancies in the $2p$ subshell of argon. The experimental results are compared to multiconfigurational Dirac-Fock (MCDF) calculations in order to provide first estimates on such correlated cross sections in complex (many-electron) systems. SPDI of few-electron systems, such as helium, is believed to be well described by nonperturbative approaches such as time-dependent close coupling [20], convergent close coupling [21], and hyperspherical R -matrix methods [22]. These advanced calculational schemes have, however, not yet been extended to the SPDI of many-electron systems with several final states and with strong correlation in the remaining photoion.

II. EXPERIMENTAL DETAILS

The experiments were carried out at the BESSY II synchrotron radiation facility, at beam-line U49/2-PGM-1, when the electron storage ring was operated in single bunch mode, delivering light pulses approximately every 800.5 ns. The working principles of the time-of-flight magnetic bottle electron spectrometer used in the experiments have been described elsewhere [2] and so we will only give a brief description here. Commercially available argon gas was let into the vacuum system through a thin stainless steel needle oriented perpendicular to the light polarization axis and the light propagation direction. Photo- and Auger electrons emitted in nearly any direction from the interaction region are trapped by the magnetic field of a nearby conical soft iron pole piece (~ 0.8 T at the pole face) attached to a cylindrical NedFeB permanent magnet and guided into an ~ 2.2 m long drift tube. A weak (few mT) homogeneous field ensures that electrons are

*Corresponding authors: per.linusson@fysik.su.se, raimund.feifel@physics.uu.se

not lost at the chamber walls and instead must follow spiraling trajectories around the magnetic field lines before reaching an MCP detector placed at the end of the drift tube, where their arrival time relative to the ionizing light pulse is recorded. Time-to-energy conversion was calibrated using photoelectron and Auger lines from Xe and Ar [23,24]. In the measurements a mechanical chopper [25] was used to reduce the frequency of the synchrotron light pulses from ~ 1.249 MHz to ~ 80 kHz. The reduced light pulse frequency means that even the time of flight of single electrons with near-zero kinetic energy, which take microseconds to reach the detector, can be referenced to the correct ionizing light pulse. The electron counting rate in the measurements was kept at approximately 2 kHz, i.e., at a fraction of 1/40 of the light pulse frequency.

III. THEORY AND COMPUTATIONS

Little is known so far about the simultaneous ionization of two electrons in a weak photon field. Formally, this process has to be described by means of second-order (or even higher-order) perturbation theory and requires that, apart from the electron-photon interaction, at least *one* additional electron-electron repulsion term is taken into account to mediate the process. Such a perturbative approach appears necessary especially if both emitted electrons arise from inner shells. From an alternative viewpoint, a major part of the correlated motion among the bound-state electrons, that leads to the double ionization, can be treated also as *relaxation* of the bound electron density as long as a large fraction of the excess energy of the photoionization is carried away by one of the electrons. Until the present, no complete second-order perturbation computation has been carried out for complex atoms in which the two-electron continuum is treated explicitly in the wave-function expansion.

As described in Eqs. (1) and (2) of Ref. [11], the cross sections for a simultaneous ionization of two electrons is most easily expressed in terms of the (electric-dipole) amplitudes,

$$D(\omega; \gamma_f J_f P_f, \epsilon_1 \kappa_1, \epsilon_2 \kappa_2 : \gamma_i J_i P_i), \quad (1)$$

which relates the initial state $|\psi_i\rangle \equiv |\psi(\gamma_i J_i P_i)\rangle$ with some allowed final state $|\psi(\gamma_f J_f P_f)\rangle$ of the (doubly ionized) photoion and the two photoelectrons in the continuum. In this brief notation of the double photoionization (amplitudes), all atomic bound states $|\psi(\gamma J P)\rangle$ are assumed to have a well-defined total energy E as well as total angular momentum J and parity P , while the photoelectrons are described by partial waves that carry away the kinetic energies ϵ_1 and ϵ_2 , respectively. Since only the sum of these energies, $\epsilon_1 + \epsilon_2 = E_i + \omega - E_f$, is determined by the energy of the incident photon, final scattering states $|\psi_i\rangle \equiv |\gamma_f J_f P_f, \epsilon_1 \kappa_1, \epsilon_2 \kappa_2 : \gamma_i J_i P_i\rangle$ need to be constructed for the evaluation of the (double) photoionization amplitudes (1). These amplitudes are the building blocks to estimate the cross sections and relative intensities (as well as their angular distribution and the properties of the photoion [26]), and to compare them with the observed spectra.

Because of the different electronic structure of the photoion in its initial and final state, however, the photoionization amplitude (1) is (almost) zero in all simple computational models. Strictly speaking, these amplitudes become

nonzero only in second-order perturbation theory if the (single-)electron-photon interaction operator is augmented by an additional electron-electron interaction (on either side of the perturbation expression). In order to avoid the summation over a complete spectrum of many-electron scattering states in such a second- or higher-order perturbation approach, we made use of the relaxation of the bound-state density by performing an independent optimization for the initial and final ionic states of the photoion. This approach appears justified to calculate the relative intensities as long as the observed spectra do not strongly depend on the kinetic-energy sharing between the electrons. For an exact representation of the initial and final states, such a *relaxation model* would be equivalent to a full second-order computation, if averaged over the kinetic energies of the two emitted electrons.

In the present work, we follow Ref. [11] and describe all atomic (bound) states by means of MCDF wave functions. In the MCDF method an atomic state is approximated by a linear combination of configuration state functions (CSF) of the same symmetry [27,28],

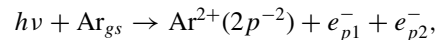
$$|\psi_\alpha(PJ)\rangle = \sum_{r=1}^{n_c} c_r(\alpha) |\gamma_r PJ\rangle, \quad (2)$$

where n_c denotes the number of CSF and $c_r(\alpha)$ the representation of the atomic state in the given basis. To generate all bound states, we applied the wave functions from the well-known GRASP92 code [29] and used the RATIP program [30] in order to evaluate the dipole amplitudes (1) from above. To account for the incomplete orthogonality of the initial- and final-state orbitals, use was made of Löwdin's expressions [31] as implemented recently in the (PHOTO component of the) RATIP program [32].

To construct the bound-state wave functions for argon in its ground and the $2p^{-2}$ doubly ionized states, we started from the $2p^6 3s^2 3p^6$ and $2p^4 3s^2 3p^6$ reference configurations for which the bound-state orbitals were optimized separately. We also included single and double excitation to define an orbital basis for the computation of the photoionization amplitudes. The main focus was placed however to allow two (quasi-)free electrons. Owing to the restricted computational model for the ionic states, the energies of the predicted photoionization peaks need to be shifted by a few eV as explained below in order to be compared with observations. For the $2p^4 3s^2 3p^6 (\epsilon_1 \kappa_1)(\epsilon_2 \kappa_2)$ final scattering states, only states with $J = 1$ were taken into account in line with the electric dipole ($E1$) approximation and its coupling to the 1S_0 ground state of argon.

IV. RESULTS AND DISCUSSION

The main process investigated in our magnetic bottle experiment, and by means of the MCDF calculations, is the simultaneous emission of two electrons from the $2p$ core orbitals; it can be written as



where e_p^- denotes a photoelectron. As the two photoelectrons may share the excess energy in a continuous fashion it is necessary to measure the sum of the kinetic energies of the photoelectron pair in order to determine the spectrum of $2p^{-2}$

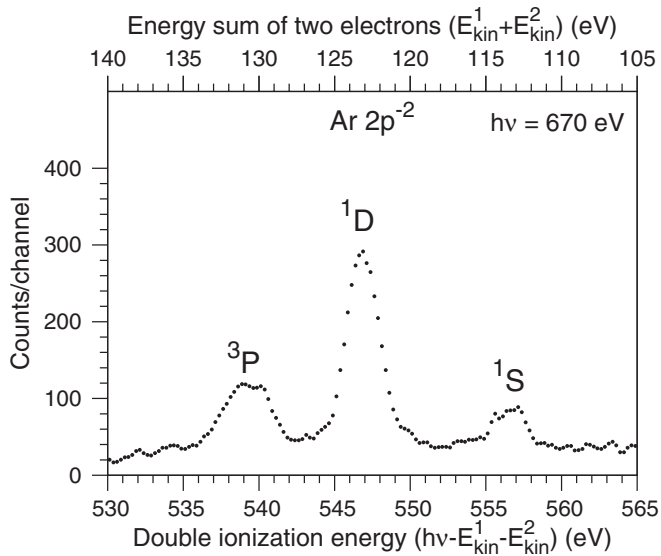
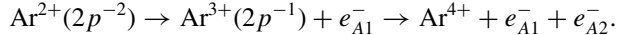


FIG. 1. Experimental spectrum of argon doubly ionized by 670 eV photons where the two electrons were removed from the $2p$ subshell.

doubly ionized states of argon. A DCH state is highly excited and decays by either electron or photon emission and with strong preference for electron emission in the case of light and medium-heavy elements. The main decay pathway of a DCH is expected to be sequential Auger decay [14,15], which in the present case can be written as



The coincident recording of all electrons emitted in the formation and decay of a $2p^{-2}$ doubly ionized state enables us, in the analysis of the experimental data, to distinguish the photoelectrons from the background of other events by filtering the data on the Auger electrons released in the decay of the $2p^{-2}$ states.

The experimental argon $2p^{-2}$ spectrum recorded at a photon energy of 670 eV is shown in Fig. 1. In order to generate this spectrum, we have analyzed quadruple electron coincidences and selected those events where one electron has a kinetic energy in the range 190 to 230 eV and another an energy in the range 140 to 195 eV. The choice of energy ranges can be understood from Figs. 2(a) and 2(b), where the spectrum of Auger electrons associated with the decay of the $2p^{-2}$ states and the spectrum of the final Ar^{4+} states are shown.

Three peaks are clearly discernible in Fig. 1 and can be attributed to the 3P , 1D , and 1S $2p^{-2}$ double hole states of argon. Since the fine structure of the 3P term is not resolved, a broad and asymmetric peak occurs at a binding energy of 540 eV; cf. Fig. 1. Because of the nonlinear background, however, no attempt was made to fit separate peaks to this structure in order to resolve the fine structure of the 3P term. The ratio of $2p^{-2}$ events to $2p^{-1}$ events in the experiment was $2.6 \pm 0.4 \times 10^{-3}$.

In Fig. 3(a) we show the energy distribution of electrons released in the formation of the 1D state. Only the energy distribution of the less energetic one of the two electrons is shown in the spectrum as the sum of kinetic energies is constant for both electrons and, hence, the distribution is symmetric around equal energy sharing. To explore the

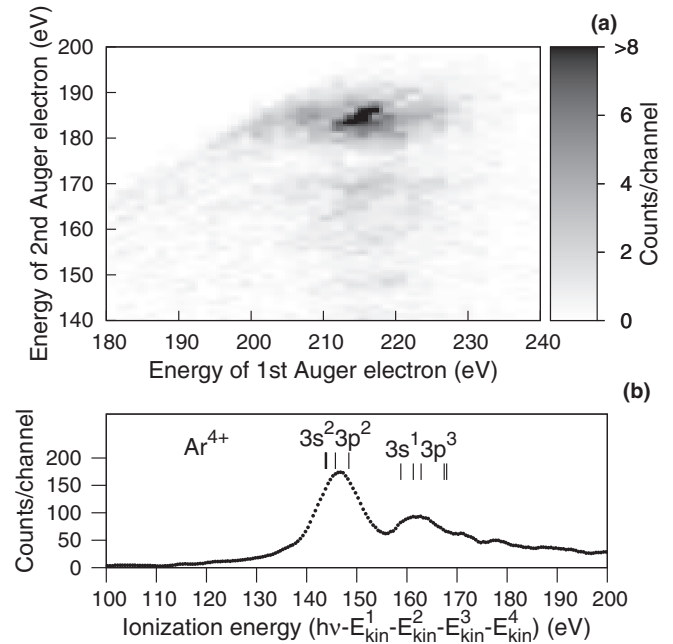


FIG. 2. (a) Coincidence map showing the energy correlation of the two Auger electrons emitted in the decay of the $2p^{-2}$ states. (b) Spectrum of the final Ar^{4+} states. Levels related to the $3s^2 3p^2$ and $3s^1 3p^3$ configurations given in the NIST database [33] are indicated by vertical bars.

direct double-ionization process, it is important to understand whether indirect channels make a significant contribution to the intensity. Such indirect channels would be visible as peaks in the energy distribution. In Fig. 3(a) background events account for the doublet structure around 15 eV, and the overall distribution is quite flat and indicates that the major contribution to the intensity is direct double ionization. Since the statistics are quite poor, the possibility for an ionization via intermediate states cannot be fully excluded if these states are sufficiently dense and, thus, appear as continuum in Fig. 3(a). In practice all possible candidates for intermediate states that are energetically suitable appear relatively exotic and include, for example, the singly ionized Rydberg states based on a

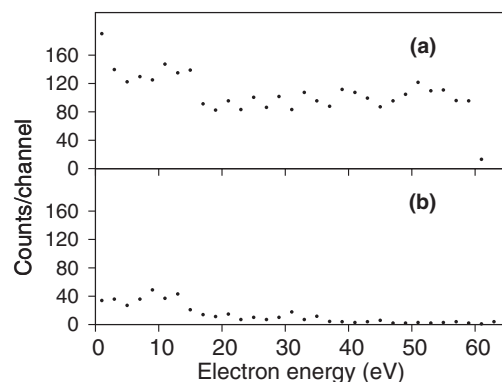


FIG. 3. (a) Energy distribution of one electron from the pair emitted in the formation of the $\text{Ar } 2p^{-2} \ ^1D$ state. (b) Spectrum of background events contaminating both (a) and the full $2p^{-2}$ spectrum (cf. Fig. 1).

TABLE I. Experimental argon $2p^{-2}$ ionization energies and relative intensities.

Assignment	Peak center (eV)	Peak area (arb. units)
3P	539.2	2.2
1D	546.9	5.2
1S	556.6	1.0

$2s^{-1}2p^{-1}$ or $2p^{-2}$ core. However, in studies of core-valence ionization in neon [8,34], indirect channels that interfere with the direct SPDI process have been shown to be of some importance. Less is known about the influence of indirect pathways on SPDI leading to double core vacancies as the few PES studies that exist so far have not been able to give clear answers on this issue. Evidently, further experimental effort is required, providing data with both better signal-to-noise ratios and higher resolution.

Ionization energies and relative intensities of the 3P , 1D , and 1S states derived from the experimental spectrum are given in Table I. The energy splittings between the 3P , 1D , and 1S states found in the present work are in good agreement with previous K - LL Auger measurements [35]. Of special interest are the intensity ratios of 2.2:5.2:1 for the $^3P : ^1D : ^1S$ states which can be compared with the statistical ratios, i.e., 9 : 5 : 1. From this comparison, we find that the ratio of the intensities of the singlet states, 1D and 1S , is quite close to the statistical weights, while the intensity of the 3P state is deficient. A strong peak corresponding to the 1D state has been noted before, in the valence np^{-2} SPDI of the rare gases [2,36] at near to moderate photon energies above threshold, as well as in $2p^{-2}$ ionization of sulfur-containing molecules [16].

In the case of valence double ionization this finding has been discussed in view of the (extended) Wannier theory [37,38], which predicts that the 1D state is suppressed, compared to the 3P state, due to the correlations and the allowed (spatial) symmetry of the escaping electron pair in the final state. In this work, the conditions are quite far from the Wannier conditions, because of the high photon energy, so that we expect that propensity of the possible states should derive from other sources. The results presented here are therefore complementary to the valence SPDI measurements and support the notion [5] that if the immediate threshold region is excluded, as a rule of thumb singlet states are favored in np^{-2} SPDI.

In Figs. 4(a) and 4(b) we show the results of the MCDF calculations for the relative intensities of a direct SPDI process. These intensities are obtained by convoluting the “bar” intensities for the electron emission into various important (double) continua with a sum of Gaussian functions in order to approximate the experimental resolution. In these figures, the calculated energies have been shifted by 4.6 eV and normalized in intensity to obtain (maximum) overlap between the calculated and experimental spectra for the 1D peak. As seen in Figs. 4(a) and 4(b) the calculated energy splittings between the 3P , 1D , and 1S double hole states are somewhat larger than those extracted from the experiment, but clearly sufficient for comparison with the corresponding peaks in the experimental spectrum. Different computational models have been applied in Figs. 4(a) and 4(b) in order to explore the role of

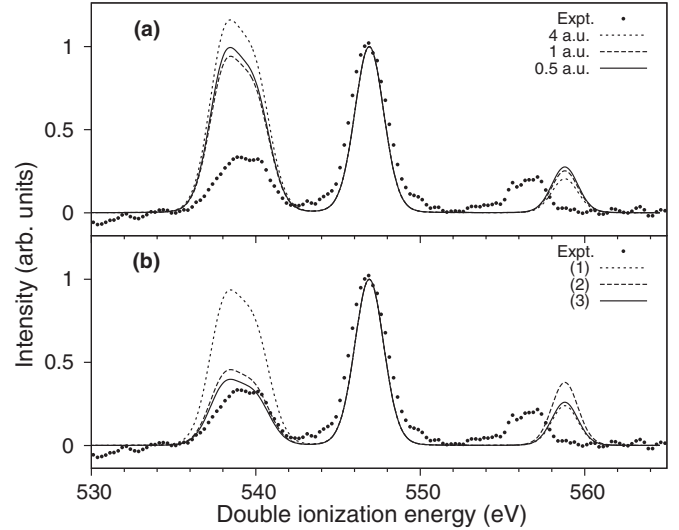


FIG. 4. (a) Calculated spectra for different sharing of the excess energy between the two photoelectrons (see text). (b) Calculated spectra for different sizes of the CSF basis in the MCDF calculations. (1) $2p^43s^23p^6$ single-configuration representation of the bound state of the remaining photoion; (2) including, in addition, $2p^2 \rightarrow 3d^2$ excitations but by restricting the scattering states to d electrons in the continuum; (3) the same as (2) for $\epsilon s + \epsilon p + \epsilon d + \epsilon f$ continua of the outgoing electrons.

the energy sharing between the two emitted electrons as well as the size of the computational basis upon the relative intensities.

In Fig. 4(a) we display the simulated spectra of the three $^3P : ^1D : ^1S$ peaks for three different energy sharings between the two emitted electrons. In these computations, the “first” electron was assumed to have kinetic energies of 4, 1, and 0.5 a.u. (with 1 a.u. = 27.21 eV), while the energy of the second electron is determined by energy conservation. Despite the rather strong separation between a fast (4 a.u. \approx 109 eV) and slow electron, the simulated spectra are not very sensitive to the energy sharing, although the intensity of the 3P peak is clearly overestimated. From further test computation, it was found that this large intensity of the 3P peak arises mainly from the (very approximate) $2p^43s^23p^6$ single-configuration representation of the 3P , 1D , and 1S terms of the photoion. Clearly improved relative intensities are obtained if $2p^2 \rightarrow 3d^2$ double excitations are taken into account, i.e., if the final scattering states are described by a linear combination of (antisymmetrized) product states of the type

$$2p^43s^23p^6(\epsilon l) \times (\epsilon' l') + 2p^23s^23p^63d^2(\epsilon l) \times (\epsilon' l'),$$

all with $J = 1$ owing to the $E1$ approximation and where $l, l' = s, p, d, f$. Unfortunately, the size of the wave-function expansions increases so rapidly that we needed to omit small contributions and that only selected excitations could be taken into account at a given time. Therefore, final conclusions about the relative importance of inner- and valence-shell contributions to the single-photon double ionization cannot be given at present. Figure 4(b) shows the simulated spectra for three different expansions of increasing complexity; see figure caption for further explanations. Though a final convergence of the predicted intensities cannot be shown, this figure indicates

that only a sufficient size of the many-electron basis allows sensible predictions on the double ionization.

V. SUMMARY AND CONCLUDING REMARKS

To summarize, we have examined the photoionization of argon leading to doubly ionized states with two vacancies in the $2p$ subshell, using the time-of-flight magnetic bottle technique. The experimental spectrum shows three peaks at 539.2, 546.9, and 556.6 eV ionization energy, which can be unambiguously assigned to the 3P , 1D , and 1S states of the $2p^{-2}$ double core hole, with relative intensities of 2.2, 5.2, and 1.0, respectively. We have also calculated the formation of $2p^{-2}$ states of argon within the framework of the MCDF method. Reasonable agreement between the observed and simulated spectra is obtained for a sufficiently large expansion of the bound-state electron density and if all partial waves including d and f electrons are taken into account in the coupling of the two outgoing electrons. For a more detailed description, it is desirable to develop a complete second-order perturbation approach that treats the bound and free electrons on an equal footing. As a first step, a representation of the (one-electron)

scattering states has been realized in the RATIP program [32] which can be utilized to evaluate (double-) ionization cross sections as well as angular distributions. Apart from the relative intensities, further investigations should consider also the energy sharing between the simultaneously emitted electrons and, if possible, their angular distribution as a function of kinetic energies.

ACKNOWLEDGMENTS

This work has been financially supported by the Swedish Research Council (VR), the Göran Gustafsson Foundation (UU/KTH), and the Knut and Alice Wallenberg Foundation, Sweden. We would like to warmly acknowledge the support by the staff and colleagues at BESSY II, Berlin. This work was also supported by the European Community–Research Infrastructure Action under the FP6 “Structuring the European Research Area” Programme (through the Integrated Infrastructure Initiative “Integrating Activity on Synchrotron and Free Electron Laser Science,” Contract No. R II 3-CT-2004-506008).

-
- [1] R. I. Hall, A. McConkey, K. Ellis, G. Dawber, L. Avaldi, M. A. MacDonald, and G. C. King, *Meas. Sci. Technol.* **3**, 316 (1992).
- [2] J. H. D. Eland, O. Vieuxmaire, T. Kinugawa, P. Lablanquie, R. I. Hall, and F. Penent, *Phys. Rev. Lett.* **90**, 053003 (2003).
- [3] P. Bolognesi, G. C. King, and L. Avaldi, *Rad. Phys. Chem.* **70**, 207 (2004).
- [4] G. C. King and L. Avaldi, *J. Phys. B: At. Mol. Opt. Phys.* **33**, R215 (2000).
- [5] J. H. D. Eland, *Adv. Chem. Phys.* **141**, 103 (2009).
- [6] E. Andersson, M. Stenrup, J. H. D. Eland, L. Hedin, M. Berglund, L. Karlsson, Å. Larson, H. Ågren, J.-E. Rubensson, and R. Feifel, *Phys. Rev. A* **78**, 023409 (2008).
- [7] T. Kaneyasu, Y. Hikosaka, E. Shigemasa, P. Lablanquie, F. Penent, and K. Ito, *J. Phys. B: At. Mol. Opt. Phys.* **41**, 135101 (2008).
- [8] Y. Hikosaka, T. Aoto, P. Lablanquie, F. Penent, E. Shigemasa, and K. Ito, *Phys. Rev. Lett.* **97**, 053003 (2006).
- [9] J. Niskanen, V. Carravetta, O. Vahtras, H. Ågren, H. Aksela, E. Andersson, L. Hedin, P. Linusson, J. H. D. Eland, L. Karlsson, J.-E. Rubensson, and R. Feifel, *Phys. Rev. A* **82**, 043436 (2010).
- [10] J. Niskanen, E. Andersson, J. H. D. Eland, P. Linusson, L. Hedin, L. Karlsson, R. Feifel, and O. Vahtras, *Phys. Rev. A* **85**, 023408 (2012).
- [11] E. Andersson, P. Linusson, S. Fritzsche, L. Hedin, J. H. D. Eland, L. Karlsson, J.-E. Rubensson, and R. Feifel, *Phys. Rev. A* **85**, 032502 (2012).
- [12] M. Mucke, J. Eland, O. Takahashi, P. Linusson, D. Lebrun, K. Ueda, and R. Feifel, *Chem. Phys. Lett.* **558**, 82 (2013).
- [13] Y. Hikosaka, P. Lablanquie, F. Penent, T. Kaneyasu, E. Shigemasa, J. H. D. Eland, T. Aoto, and K. Ito, *Phys. Rev. Lett.* **98**, 183002 (2007).
- [14] J. H. D. Eland, M. Tashiro, P. Linusson, M. Ehara, K. Ueda, and R. Feifel, *Phys. Rev. Lett.* **105**, 213005 (2010).
- [15] P. Lablanquie, F. Penent, J. Palaudoux, L. Andric, P. Selles, S. Carniato, K. Bučar, M. Žitnik, M. Huttula, J. H. D. Eland, E. Shigemasa, K. Soejima, Y. Hikosaka, I. H. Suzuki, M. Nakano, and K. Ito, *Phys. Rev. Lett.* **106**, 063003 (2011).
- [16] P. Linusson, O. Takahashi, K. Ueda, J. H. D. Eland, and R. Feifel, *Phys. Rev. A* **83**, 022506 (2011).
- [17] P. Lablanquie, T. P. Grozdanov, M. Žitnik, S. Carniato, P. Selles, L. Andric, J. Palaudoux, F. Penent, H. Iwayama, E. Shigemasa, Y. Hikosaka, K. Soejima, M. Nakano, I. H. Suzuki, and K. Ito, *Phys. Rev. Lett.* **107**, 193004 (2011).
- [18] J. P. Briand, P. Chevallier, M. Tavernier, and J. P. Rozet, *Phys. Rev. Lett.* **27**, 777 (1971).
- [19] S. H. Southworth, E. P. Kanter, B. Krässig, L. Young, G. B. Armen, J. C. Levin, D. L. Ederer, and M. H. Chen, *Phys. Rev. A* **67**, 062712 (2003).
- [20] J. Colgan, M. S. Pindzola, and F. Robicieux, *J. Phys. B: At. Mol. Opt. Phys.* **34**, L457 (2001).
- [21] A. S. Kheifets and I. Bray, *Phys. Rev. A* **54**, R995 (1996).
- [22] L. Malegat, P. Selles, and A. K. Kazansky, *Phys. Rev. Lett.* **85**, 4450 (2000).
- [23] T. X. Carroll, J. D. Bozek, E. Kukk, V. Myrseth, L. J. Sthre, T. D. Thomas, and K. Wiesner, *J. Electr. Spectrosc. Relat. Phenom.* **125**, 127 (2002).
- [24] G. C. King, M. Tronc, F. H. Read, and R. C. Bradford, *J. Phys. B* **10**, 2479 (1977).
- [25] S. Plogmaker, P. Linusson, J. H. D. Eland, N. Baker, E. M. J. Johansson, H. Rensmo, R. Feifel, and H. Siegbahn, *Rev. Sci. Instrum.* **83**, 013115 (2012).
- [26] N. Kabachnik, S. Fritzsche, A. Grum-Grzhimailo, M. Meyer, and K. Ueda, *Phys. Rep.* **451**, 155 (2007).

- [27] I. P. Grant, *Methods in Computational Chemistry*, edited by S. Wilson (Plenum Press, New York, 1988).
- [28] S. Fritzsche, *Phys. Scr. T* **100**, 37 (2002).
- [29] F. A. Parpia, C. Froese Fischer, and I. P. Grant, *Comput. Phys. Commun.* **94**, 249 (1996).
- [30] S. Fritzsche, *J. Electr. Spectrosc. Relat. Phenom.* **114-116**, 1155 (2001).
- [31] P.-O. Löwdin, *Phys. Rev.* **97**, 1474 (1955).
- [32] S. Fritzsche, *Comput. Phys. Commun.* **183**, 1525 (2012).
- [33] Y. Ralchenko, A. Kramida, J. Reader, and NIST ASD Team (2010), *NIST Atomic Spectra Database* (ver. 4.0.1) (online). Available at <http://physics.nist.gov/asd> (National Institute of Standards and Technology, Gaithersburg, MD, 2013).
- [34] S. Svensson, N. Mårtensson, and U. Gelius, *Phys. Rev. Lett.* **58**, 2639 (1987).
- [35] L. Asplund, P. Kelfve, B. Blomster, H. Siegbahn, and K. Siegbahn, *Phys. Scr.* **16**, 268 (1977).
- [36] L. Avaldi, G. Dawber, N. Gulley, H. Rojas, G. C. King, R. Hall, M. Stuhel, and M. Zitnik, *J. Phys. B: At. Mol. Opt. Phys.* **30**, 5197 (1997).
- [37] G. H. Wannier, *Phys. Rev.* **90**, 817 (1953).
- [38] A. Huetz, P. Selles, D. Waymel, and J. Mazeau, *J. Phys. B: At. Mol. Opt. Phys.* **24**, 1917 (1991).